

## A green, solvent-free route to functionalised metal-organic frameworks with UiO-66 topology

Roberto D'Amato,<sup>a</sup> Fabio Marmottini,<sup>a</sup> Matthew J. McPherson,<sup>b</sup> Marco Taddei<sup>\*,b</sup> and Ferdinando Costantino<sup>\*,a</sup>

Received 00th January 20xx,  
Accepted 00th January 20xx

DOI: 10.1039/x0xx00000x

www.rsc.org/

**We report a solvent-free procedure for the high-yield synthesis of metal-organic frameworks of UiO-66 topology starting from a range of commercial Zr(IV) precursors and various substituted dicarboxylic linkers. The syntheses are carried out by simply grinding the reagents in the presence of a small volume of acetic acid as modulator, followed by incubation at either room temperature or 120 °C. Use of a ball mill for the grinding step is demonstrated to enable facile scale up of the synthesis. High acidity of the linker is found to be a crucial factor in affording materials of quality comparable to that of products obtained in solvo- or hydrothermal conditions.**

The development of green and scalable procedures for the synthesis of metal-organic frameworks (MOFs) is currently considered the main factor to enable widespread industrial application and commercialization of these materials.<sup>1,2</sup> Scientific attention is mainly focussed on the production of highly stable MOF at low cost, in high yield and fulfilling the requirements of sustainability and green chemistry principles.<sup>3,4</sup> Zirconium-based MOFs (Zr-MOFs) are currently considered benchmark materials for their high chemical and thermal stability, structural versatility and employment in a vast range of applications, ranging from gas separation,<sup>5-7</sup> catalysis,<sup>8,9</sup> water sorption,<sup>10,11</sup> proton conductivity<sup>12</sup> and drug delivery.<sup>13</sup> Their structure is based on the different connectivity of hexanuclear clusters of formula  $Zr_6O_6(OH)_4^{12+}$  with polytopic carboxylic linkers, designing MOFs with variable degrees of connectivity and topologies, such as **fcu** (UiO-66 and MOF-801), **csq** (NU-1000) and **spn** (MOF-808).<sup>14-17</sup> Zr-MOFs are often prepared employing high boiling hazardous solvents such as *N,N*-dimethylformamide (DMF), strong acids and soluble chloride or nitrate metal salts.<sup>18</sup> A remarkable effort has been recently made for ensuring safer and cleaner procedures for the synthesis of MOFs by using different approaches able to

minimize the use of hazardous reagents and high-boiling solvents and the generation of large amounts of waste byproducts.<sup>19</sup> Mechanochemistry is a well-established approach for performing clean and fast syntheses of a wide range of compounds, including metal-organic materials, avoiding common solvothermal routes and maximizing the atom economy.<sup>20</sup> In particular, liquid assisted grinding (LAG) or ionic-liquid assisted grinding (ILAG) are efficient procedures that make use of a small amount of solvents and/or metal-oxide precursors to enhance the crystallization kinetics.<sup>21-23</sup> Mechanochemical routes have recently been developed for the synthesis of many Zr-MOFs.<sup>24</sup> In particular, the use of templating agents, water-based LAG and extrusion resulted in the synthesis of Zr-MOFs of different topologies with high yield and high purity.<sup>25</sup> However, in order to attain the desired phase, preformed  $Zr_6O_6(OH)_4^{12+}$  clusters already assembled with monocarboxylic ligands, such as acetate or methacrylate, are normally used.<sup>25,26</sup> These clusters are often prepared using wet chemistry routes, adding a preliminary synthetic step to the procedure. Huang et al.<sup>24</sup> recently reported the ultrarapid (3 min) water-based LAG synthesis of nanocrystalline perfluorinated UiO-66 starting from a preformed methacrylate cluster and tetrafluoroterephthalic acid ( $F_4$ -BDC). The authors found that other linkers, such as terephthalic acid (BDC), 2-aminoterephthalic acid ( $NH_2$ -BDC) and 2-bromoterephthalic acid (Br-BDC) failed to afford a crystalline product, attributing the higher reactivity of  $F_4$ -BDC to its higher acidity, which enhances its solubility in water. Indeed,  $F_4$ -BDC has recently been employed for the synthesis of UiO-66 type MOFs in water, even at room temperature.<sup>27-30</sup> Notably, Ye et al.<sup>31</sup> recently reported on a simple method to produce UiO-66 in high yield by grinding  $ZrOCl_2 \cdot 8H_2O$  and BDC and subsequently heating the resulting mixture at 130 °C for 12 hours. Attempts using  $ZrCl_4$  and  $Zr(NO_3)_4 \cdot 5H_2O$  as precursors failed to afford a crystalline product. Inspired by these works, we set out to combine these two approaches to investigate the synthesis of a range of functionalised UiO-66 analogues starting from several commercially available Zr precursors, namely,  $Zr(NO_3)_4 \cdot 5H_2O$ ,  $ZrOCl_2 \cdot 8H_2O$ ,  $ZrO(NO_3)_2 \cdot 4H_2O$  and  $ZrCl_4$ , and a range of linkers

<sup>a</sup> Dipartimento di Chimica Biologia e Biotecnologia, University of Perugia, Via Elce di Sotto 8, 06123 Perugia, Italy. Email: [ferdinando.costantino@unipg.it](mailto:ferdinando.costantino@unipg.it)

<sup>b</sup> Energy Safety Research Institute, Swansea University, Fabian Way, Swansea SA1 8EN, United Kingdom. Email: [marco.taddei@swansea.ac.uk](mailto:marco.taddei@swansea.ac.uk)

with variable acidity, namely, F<sub>4</sub>-BDC, Br-BDC, NH<sub>2</sub>-BDC, 2-nitroterephthalic acid (NO<sub>2</sub>-BDC) and 2,5-pyridine dicarboxylic acid (PyDC) (Figure 1).

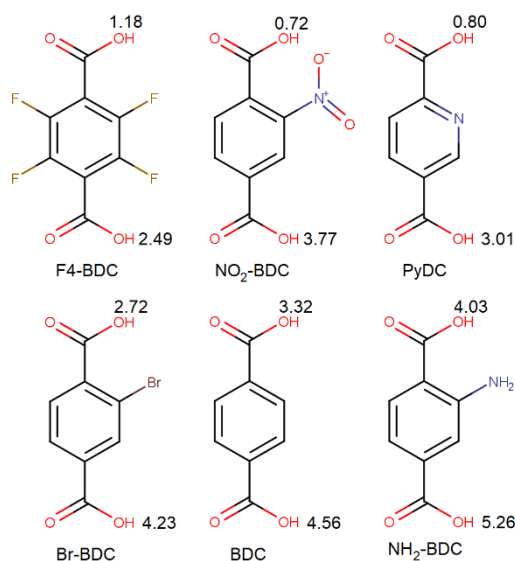


Figure 1. Molecular structure of the linkers used in this work. pKa values are also included next to the corresponding carboxylic groups. The values were calculated using the online tool *Chemicalize* ([chemicalize.com](http://chemicalize.com)).

We started our investigation by screening the different Zr precursors in combination with F<sub>4</sub>-BDC, which was demonstrated by Huang et al.<sup>27</sup> to be very prone to quick form a UiO-66 phase when milled with preformed hexanuclear Zr clusters. Initial attempts consisted in simply grinding equimolar amounts of the Zr precursor and F<sub>4</sub>-BDC (1mmol each) in a mortar in the presence of 1 mL of acetic acid (AcOH, 99.7%, 17.5 mmol) for five minutes. The resulting slurry was then transferred to a closed container and incubated at RT for 24 hours. The mixture was then washed with water to remove the unreacted Zr salts and linker and centrifuged in order to recover the solid. Using these amounts of reagents, a concentration of 1 M of both salt and linker was obtained, which is 10 to 40 times higher than that normally used for DMF- or water-based syntheses of UiO-66 type MOFs.<sup>25,29,32-34</sup> We avoided the direct addition of water as solvent since the amount needed to form the clusters (1.33 equivalents) was already present in the hydrated Zr salts used as metal source. Quite surprisingly, we obtained phase-pure and crystalline UiO-66 from Zr(NO<sub>3</sub>)<sub>4</sub>·5H<sub>2</sub>O, ZrOCl<sub>2</sub>·8H<sub>2</sub>O and ZrCl<sub>4</sub> (Figure 2a). In the case of ZrO(NO<sub>3</sub>)<sub>2</sub>·4H<sub>2</sub>O, the mixture had to be heated to 120 °C in order to obtain a crystalline product (Figure 1S). The products obtained from Zr(NO<sub>3</sub>)<sub>4</sub>·5H<sub>2</sub>O and ZrOCl<sub>2</sub>·8H<sub>2</sub>O displayed broad reflections around 4-5° 2θ, which could be associated with the presence of defects. No residual reflections of the linker were present in the products (Figure 2S). SEM micrographs show that MOF crystallites with no defined morphology and size in the nanometric range (below 100 nm) were formed (Figure 3S). Although ZrCl<sub>4</sub> is an anhydrous salt, its use was likely successful because it is highly sensitive to moisture and, during grinding, it could have absorbed water from atmosphere. The N<sub>2</sub> adsorption-desorption isotherms at 77K obtained with these

samples are reported in Figure 2b and they can be classified as type I isotherms, which are typical of microporous materials. The specific surface area and micropore volumes were calculated from the Brunauer-Emmett-Teller (BET) and t-plot analyses of the adsorption data, respectively, and are reported in Table 1. The highest BET surface area of 882 m<sup>2</sup> g<sup>-1</sup> was recorded for the sample obtained from Zr(NO<sub>3</sub>)<sub>4</sub>·5H<sub>2</sub>O. This value is higher than that previously reported for perfluorinated UiO-66 synthesized in water.<sup>25,28</sup> ZrCl<sub>4</sub> produces by far the least porous product, which could be explained by the formation of amorphous, non-porous impurities due to the lower amount of water present in this precursor, compared to the other ones.

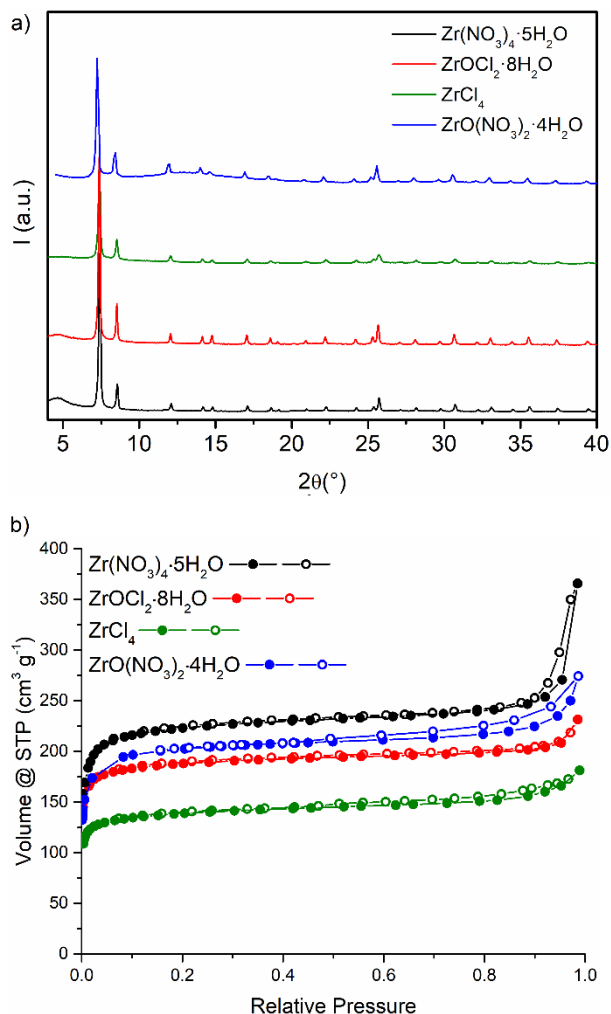


Figure 2. PXRD patterns (a) and N<sub>2</sub> adsorption isotherms at 77 K (b) of the products obtained from the reaction of F<sub>4</sub>-BDC with Zr(NO<sub>3</sub>)<sub>4</sub>·5H<sub>2</sub>O (black), ZrOCl<sub>2</sub>·8H<sub>2</sub>O (red) and ZrCl<sub>4</sub> (olive) at RT and with ZrO(NO<sub>3</sub>)<sub>2</sub>·4H<sub>2</sub>O at 120 °C (blue).

NMR analysis of the solids digested in 1 M NaOH in D<sub>2</sub>O showed that a little AcOH was retained within all the MOFs except the one prepared with ZrOCl<sub>2</sub>·8H<sub>2</sub>O, suggesting the presence of some defects (Figures 4S-7S). Thermogravimetric analysis (TGA) shows that all products start decomposing at a similar temperature of 300 °C, consistent with that observed in previous literature reports (Figure 8S).<sup>1,28</sup> The synthesis was also tried with smaller amount of AcOH (0.1 mL), using

Zr(NO<sub>3</sub>)<sub>4</sub>·5H<sub>2</sub>O as metal precursor, obtaining products with lower crystallinity (Figure 9S), suggesting that a high AcOH/Zr ratio is crucial to aid formation of metal clusters and induce formation of a well crystallised MOF. These results suggest that Zr(NO<sub>3</sub>)<sub>4</sub>·5H<sub>2</sub>O is the most suitable precursor to obtain UiO-66 with high crystallinity and porosity in mild conditions.

Table 1. BET surface area and micropore volume values for perfluorinated UiO-66 samples synthesised starting from different Zr precursors.

Precursor	Incubation temperature	BET surface area (m <sup>2</sup> g <sup>-1</sup> )	Micropore Volume (cm <sup>3</sup> g <sup>-1</sup> )
Zr(NO <sub>3</sub> ) <sub>4</sub> ·5H <sub>2</sub> O	RT	882	0.31
ZrOCl <sub>2</sub> ·8H <sub>2</sub> O	RT	750	0.27
ZrCl <sub>4</sub>	RT	540	0.19
ZrO(NO <sub>3</sub> ) <sub>2</sub> ·4H <sub>2</sub> O	120 °C	783	0.30

We then moved on to screen linkers bearing different functional groups. The same procedure described above was employed, using Zr(NO<sub>3</sub>)<sub>4</sub>·5H<sub>2</sub>O as the metal precursor and simply replacing F<sub>4</sub>-BDC with either Br-BDC, NO<sub>2</sub>-BDC, PyDC, NH<sub>2</sub>-BDC or BDC (Figure 1). Incubation of the mixture at RT only afforded a reasonably crystalline and porous UiO-66 phase for NO<sub>2</sub>-BDC (BET s.a. = 842 m<sup>2</sup> g<sup>-1</sup>, micropore volume = 0.29 cm<sup>3</sup> g<sup>-1</sup>, consistent with previous literature reports)<sup>33,34</sup> (Figure 3, Table 2). In an attempt to improve the quality of this product, we heated the mixture to 120 °C, but, quite surprisingly, this led to a less crystalline and less porous MOF (micropore volume = 0.23 cm<sup>3</sup> g<sup>-1</sup>) (Figures 10S-11S). NMR analysis shows that the products contain similar amounts of AcOH (Figures 12S-13S). Comparison of the TGA curves shows that they start decomposing at the same temperature (about 350 °C), but the one obtained at RT loses considerably less weight (Figure 14S). In the case of Br-BDC, the phase formed at RT did resemble UiO-66, but its crystallinity was clearly unsatisfactorily (Figure 15S). Heating to 120 °C was necessary to obtain a crystalline product, whose surface area (BET s.a. = 526 m<sup>2</sup> g<sup>-1</sup>) was still lower than that usually reported in the literature,<sup>32,35,36</sup> comprised between 718 and 851 m<sup>2</sup> g<sup>-1</sup> (Figure 3 b)). NMR analysis showed that the sample contained the highest amount of AcOH among all the MOFs here reported (Figure 16S). This suggests the potential presence of amorphous, non-porous impurities. In the case of PyDC, AcOH proved not to be an effective modulator in any condition, therefore addition of 1 mL of concentrated HNO<sub>3</sub> (65%) was attempted, drawing inspiration from a literature synthetic protocol, where concentrated HCl was employed to prevent the formation of an amorphous phase.<sup>37</sup> We chose to use HNO<sub>3</sub> in order to avoid the introduction of an additional species, i.e. chloride, in the reaction mixture. While incubation at RT did not succeed in affording a crystalline product (Figure 17S), heating to 120 °C did produce a highly crystalline solid, with BET s.a. of 1108 m<sup>2</sup> g<sup>-1</sup> and micropore volume of 0.41 cm<sup>3</sup> g<sup>-1</sup> (Figure 3, Table 2). This product is significantly less porous than previously reported analogues<sup>37,38</sup> with BET s.a. ranging

between 1380 and 1797 m<sup>2</sup> g<sup>-1</sup>. However, these literature samples contained large amounts of defects, which contributed to inflate their porosity. Given that PyDC and BDC have basically the same molecular weight and steric demand, a BET s.a. value of 1108 m<sup>2</sup> g<sup>-1</sup> is consistent with the values usually reported for defect-free and non-functionalised UiO-66.<sup>39</sup> However, the wt% of PyDC in the MOF derived from NMR analysis is lower than expected for a non-defective sample (Figure 18S). This could be due to the presence of either amorphous, non-porous impurities or some NO<sub>3</sub><sup>-</sup> as counterion of the protonated pyridine rings. SEM micrographs show that MOF crystallites with no defined morphology and size in the nanometric range (below 100 nm) were formed with NO<sub>2</sub>-BDC and Br-BDC, whereas PyDC gave octahedral crystallites (Figure 3S). No residual reflections of the linker were present in any of the products (Figure 2S).

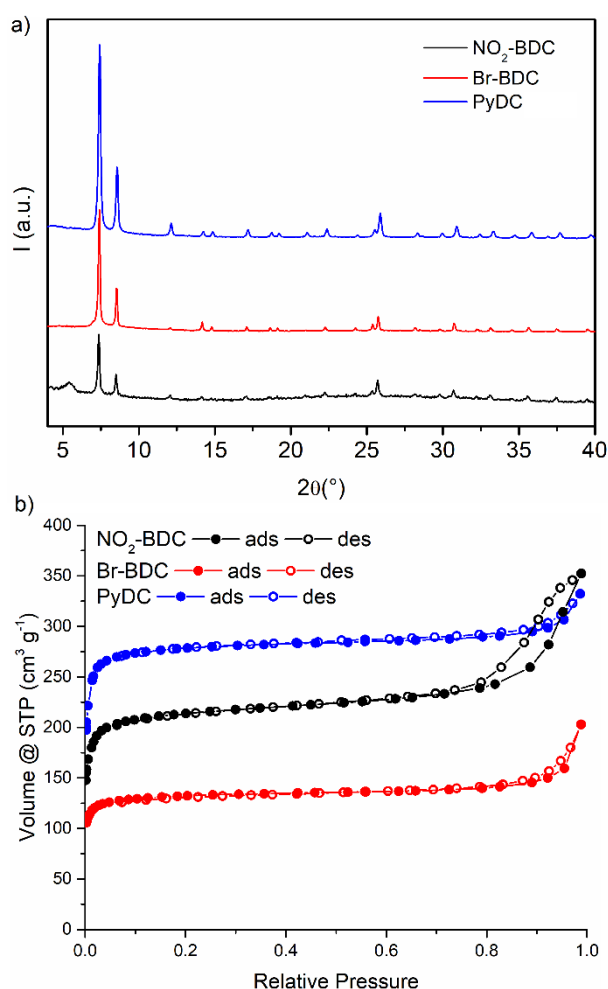


Figure 3. PXRD patterns (a) and N<sub>2</sub> adsorption isotherms at 77 K (b) of the products obtained from the reaction of Zr(NO<sub>3</sub>)<sub>4</sub>·5H<sub>2</sub>O with NO<sub>2</sub>-BDC at RT (black) and with Br-BDC (red) and PyDC (blue) at 120 °C.

Every attempt at using NH<sub>2</sub>-BDC and BDC as linkers invariably ended with an amorphous product. This is probably because these ligands are not acidic enough and therefore not able to effectively deprotonate in reaction conditions. As shown in Figure 1, pK<sub>a1</sub> values of BDC and NH<sub>2</sub>-BDC are 3.32 and 4.03,

respectively, about one order of magnitude lower than that of Br-BDC (2.72) and more than two orders of magnitude lower than those of F<sub>4</sub>-BDC (1.18), NO<sub>2</sub>-BDC (0.72), and PyDC (0.80). Since solubility in water is highly dependent on the acidity of the carboxylic linker, which is in turn related to the presence of electron-withdrawing substituents on the aromatic ring, we speculate that less acidic linkers, such as BDC and NH<sub>2</sub>-BDC, fail to dissolve in the small amount of water contained in the Zr precursor, thus preventing crystallisation of the MOF from occurring. On the other hand, the higher water solubility of F<sub>4</sub>-BDC, NO<sub>2</sub>-BDC, Br-BDC and PyDC allows the rapid reaction with hydrated Zr salts upon grinding and successive incubation at RT or 120 °C.

Table 2. BET surface area and micropore volume values for UiO-66 samples synthesised using different organic linkers.

Linker	Incubation temperature	BET surface area (m <sup>2</sup> g <sup>-1</sup> )	Micropore Volume (cm <sup>3</sup> g <sup>-1</sup> )
NO <sub>2</sub> -BDC	RT	842	0.29
Br-BDC	120 °C	526	0.18
PyDC	120 °C	1108	0.41

In order to test the possibility to scale-up the synthetic procedure, a ball mill was used for the mixing stage. The synthesis of UiO-66 using F<sub>4</sub>-BDC and Zr(NO<sub>3</sub>)<sub>4</sub>·5H<sub>2</sub>O (4 mmol each) and 4 mL of AcOH was initially tried by milling for 1 h at 30 Hz, observing formation of a UiO-66 phase with low crystallinity and porosity (Figures 19S–20S). In a successive attempt, where the vessel was kept sealed for 24 h after initial milling, 1.5 g of a well crystallized compound was obtained, whose crystallinity is comparable to that obtained by hand-grinding the reagents (Figure 19S). This product displays BET s.a. of 888 m<sup>2</sup>g<sup>-1</sup> and micropore volume of 0.33 cm<sup>3</sup> g<sup>-1</sup>, about the same of that measured for the MOF obtained with the small scale synthesis (Figure 20S). The scale of the reaction is limited by the volume (10 mL) of the vessel available to us, but the success of this four-fold scale up suggests that it could be further increased. This demonstrates that ball milling is effective for scaled-up syntheses because it allows a more efficient mixing of the reagents when they are in large amounts and hand-grinding is not practical. However, it does not appear to have evident benefits in terms of kinetics of crystallization.

## Conclusions

A novel synthetic route for Zr-MOFs with UiO-66 structure is here presented. The synthetic protocol is extremely easy as it does not make use of solvents and preformed Zr<sub>6</sub> clusters. The procedure was successfully validated with different Zr salts and dicarboxylic linkers at the laboratory scale. The protocol works best with linkers having high acidity, such as tetrafluoro-, 2-nitro- and 2-bromoterephthalic acid and 2,5-pyridinedicarboxylic acid. High acidity allows facile

deprotonation in the presence of the crystallisation water contained in the metal precursors, thus promoting formation of the Zr clusters. We also demonstrated that the use of ball mill for the grinding stage permits a four-fold scale up of the synthesis, while affording a product of identical quality.

## Acknowledgement

The authors acknowledge the European Union's Horizon 2020 research and innovation programme under the Marie Skłodowska-Curie grant agreement No 663830 (M.T.), and the Engineering and Physical Sciences Research Council (EPSRC) for funding through the First Grant scheme EP/R01910X/1 (M.T. and M.J.M.). Prof Paul M. Williams (Swansea University) is acknowledged for providing access to the gas sorption analyser.

## Conflicts of interest

There are no conflicts to declare.

## Notes and references

- H. Reinsch, *Eur. J. Inorg. Chem.*, 2016, 4290–4299.
- S. Wang and C. Serre, *ACS Sustainable Chem. Eng.*, 2019, **7**, 11911–11927.
- P. A. Julien, C. Mottillo and T. Friščić *Green Chem.*, 2017, **19**, 2729–2747.
- T. D. Bennett and S. Horike, *Nat. Rev. Mater.*, 2018, **3**, 431–440.
- K. Adil, Y. Belmabkhout, R. S. Pillai, A. Cadiau, P. M. Bhatt, A. H. Assen, G. Maurin and M. Eddaoudi, *Chem. Soc. Rev.*, 2017, **46**, 3402–3430.
- J. A. Mason, M. Veenstra and J. R. Long, *Chem. Sci.*, 2014, **5**, 32–51.
- Z. Chen, K. Adil, L. J. Weselinski, Y. Belmabkhout and M. Eddaoudi, *J. Mater. Chem. A*, 2015, **3**, 6276–6281.
- J. E. Mondloch, M. J. Katz, W. C. Isley III, P. Ghosh, P. Liao, W. Bury, G. W. Wagner, M. G. Hall, J. B. DeCoste, G. W. Peterson, R. Q. Snurr, C. J. Cramer, J. T. Hupp and O. K. Farha, *Nat. Mater.*, 2015, **14**, 512–516.
- D. Yang and B. C. Gates *ACS Catalysis*, 2019, **9**, 1779–1798.
- A. Cadiau, Y. Belmabkhout, K. Adil, P. M. Bhatt, R. S. Pillai, A. Shkurenko, C. Martineau-Corcos, G. Maurin and M. Eddaoudi, *Science*, 2017, **356**, 731–735.
- Z. Chen, P. Li, X. Zhang, P. Li, M. C. Wasson, T. Islamoglu, J. F. Stoddart and O. K. Farha, *J. Am. Chem. Soc.*, 2019, **141**, 2900–2905.
- J. Escorihuela, R. Narducci, F. Costantino and F. Companon, *Adv. Mater. Interfaces*, 2019, **6**, 1801146.
- M. X. Wu and Y. W. Yang, *Adv. Mater.*, 2017, **29**, 1606134.
- J. H. Cavka, S. Jakobsen, U. Olsbye, N. Guillou, C. Lamberti, S. Bordiga and K. P. Lillerud *J. Am. Chem. Soc.*, 2008, **130**, 13850–13851.
- O. K. Farha, A. Ö. Yazaydin, I. Eryazici, C. D. Malliakas, G. H. Brad, M. Kanatzidis, S. T. Nguyen, S. Q. Randall and J. T. Hupp, *Nature Chem.*, 2010, **2**, 944–948.
- D. Feng, Z.-Y. Gu, J.-R. Li, H.-L. Jiang, Z. Wei and H.-C. Zhou, *Angew. Chem. Int. Ed.*, 2012, **51**, 10307–10310.
- J. C. Jiang, F. Gándara, Y. B. Zhang, K. Na, O. M. Yaghi and W. G. Klemperer, *J. Am. Chem. Soc.*, 2014, **136**, 12844–12847.
- A. U. Czaja, N. Trukhan and U. Muller, *Chem. Soc. Rev.*, 2009, **38**, 1284.

- 19 Y. Bai, Y. Dou, L.-H. Xie, W. Rutledge, J.-R. Li and H.-C. Zhou, *Chem. Soc. Rev.*, 2016, **45**, 2327–2367.
- 20 T. Friščić and W. Jones, *Cryst. Growth Des.*, 2009, **9**, 1621–1637.
- 21 Beldon, P. J.; Fábián, L.; Stein, R. S.; Thirumurugan, A.; Cheetham, A. K.; Friščić, T., *Angew. Chem. Int. Ed.* 2010, **49**, 9640–9643.
- 22 S. L. James, C. J. Adams, C. Bolm, D. Braga, P. Collier, T. Friščić, F. Grepioni, K. D. M. Harris, G. Hyett, W. Jones, A. Krebs, J. Mack, L. Maini, A. G. Orpen, I. P. Parkin, W. C. Shearouse, J. W. Steed and D. C. Waddell, *Chem. Soc. Rev.*, 2012, **41**, 413–447.
- 23 Julien, P. A.; Užarević, K.; Katsenis, A. D.; Kimber, S. A. J.; Wang, T.; Farha, O. K.; Zhang, Y.; Casaban, J.; Germann, L. S.; Etter, M.; et al, *J. Am. Chem. Soc.*, 2016, **138** (9), 2929–2932.
- 24 Y.-H. Huang, W.-S. Lo, Y.-W. Kuo, W.-J. Chen, C.-H. Lin, F.-K. Shieh, *Chem. Commun.*, 2017, **53**, 5818–5821.
- 25 B. Karadeniz, A. J. Howarth, T. Stolar, T. Islamoglu, I. Dejanović, M. Tireli, M. C. Wasson, S.-Y. Moon, O. K. Farha, T. Friščić and K. Užarević, *ACS Sustainable Chem. Eng.*, 2018, **6**, 15841–15849.
- 26 K. Užarević, T.C. Wang, S.-Y. Moon, A. M. Fidelli, J.T. Hupp, O. K. Farha and T. Friščić, *Chem. Commun.*, 2016, **52**, 2133–2136.
- 27 H. Reinsch, B. Bueken, F. Vermoortele, I. Stassen, A. Lieb, K.-P. Lillerund and D. De Vos, *CrystEngComm*, 2015, **17**, 4070–4074.
- 28 Z. Chen, X. Wang, H. Noh, G. Ayoub, G. W. Peterson, C. T. Buru, T. Islamoglu and O. K. Farha, *CrystEngComm*, 2019, **21**, 2409–2415.
- 29 Z. Hu, A. Gami, Y. Wang and D. Zhao, *Adv. Sustainable Syst.*, 2017, **1**, 1700092–1700104.
- 30 R. D’Amato, A. Donnadio, M. Carta, C. Sangregorio, D. Tiana, R. Vivani, M. Taddei and F. Costantino, *ACS Sustainable Chem. Eng.*, 2019, **7**, 394–402.
- 31 G. Ye, D. Zhang, X. Li, K. Leng, W. Zhang, J. Ma, Y. Sun, W. Xu and S. Ma, *ACS Appl. Mater. Interfaces*, 2017, **9**, 34937–34943.
- 32 M. Taddei, D. Tiana, N. Casati, J. A. van Bokhoven, B. Smit and M. Ranocchiari, *Phys. Chem. Chem. Phys.*, 2017, **19**, 1551–1559.
- 33 M. Taddei, R. J. Wakeham, A. Koutsianos, E. Andreoli and A. R. Barron, *Angew. Chem. Int. Ed.*, 2018, **57**, 11706–11710.
- 34 M.J. Katz, Z. J. Brown, Y. J. Colon, P.I.W. Siu, K. A. Scheidt, R.Q. Snurr, J. T. Hupp and O. K. Farha, *Chem. Commun.*, 2013, **49**, 9449–9451.
- 35 M. Kandiah, M. H. Nilsen, S. Usseglio, S. Jakobsen, U. Olsbye, M. Tilset, C. Larabi, E.A. Quadrelli, F. Bonino and K.P. Lillerud, *Chem. Mater.*, 2010, **22**, 6632–6640.
- 36 S. J. Garibay and S. M. Cohen, *Chem. Commun.*, 2010, **41**, 7700–7702.
- 37 A. A. Barkhordarian and C. J. Kepert, *J. Mater. Chem. A*, 2017, **5**, 5612–5618.
- 38 S. Waitschat, D. Fröhlich, H. Reinsch, H. Terraschke, K. A. Lomachenko, C. Lamberti, H. Kummer, T. Helling, M. Baumgartner, S. Henninger and N. Stock, *Dalton Trans.*, 2018, **47**, 1062–1070.
- 39 G. C. Shearer, S. Chavan, S. Bordiga, S. V. Velle, U. Olsbye and K. P. Lillerud, *Chem. Mater.*, 2016, **28**, 3749–3761.